



A mechanistic model for the prediction of cutting forces in the face-milling of ductile spheroidal cast iron components for wind industry application

Checchi, Alessandro; Bissacco, Giuliano; Hansen, Hans Nørgaard

Published in:
Procedia CIRP

Link to article, DOI:
[10.1016/j.procir.2018.09.003](https://doi.org/10.1016/j.procir.2018.09.003)

Publication date:
2018

Document Version
Publisher's PDF, also known as Version of record

[Link back to DTU Orbit](#)

Citation (APA):

Checchi, A., Bissacco, G., & Hansen, H. N. (2018). A mechanistic model for the prediction of cutting forces in the face-milling of ductile spheroidal cast iron components for wind industry application. *Procedia CIRP*, 77, 231-234. <https://doi.org/10.1016/j.procir.2018.09.003>

General rights

Copyright and moral rights for the publications made accessible in the public portal are retained by the authors and/or other copyright owners and it is a condition of accessing publications that users recognise and abide by the legal requirements associated with these rights.

- Users may download and print one copy of any publication from the public portal for the purpose of private study or research.
- You may not further distribute the material or use it for any profit-making activity or commercial gain
- You may freely distribute the URL identifying the publication in the public portal

If you believe that this document breaches copyright please contact us providing details, and we will remove access to the work immediately and investigate your claim.

8th CIRP Conference on High Performance Cutting (HPC 2018)

A mechanistic model for the prediction of cutting forces in the face-milling of ductile spheroidal cast iron components for wind industry application

Alessandro Checchi*, Giuliano Bissacco, Hans Nørgaard Hansen

Technical University of Denmark DTU, Department of Mechanical Engineering, Produktionstorvet Building: 427, Kgs. Lyngby, 2800, Denmark

* Corresponding author. Tel.: +45 45254834. E-mail address: aleche@mek.dtu.dk

Abstract

Among renewable energy sources, wind energy has received considerable impulse in the last decade. Not only the number of manufactured wind turbines is raising, but also the overall size of the components is increasing, for improved energy harvesting. The increase of hub dimensions implies the need for larger, tailor built, milling machines, with impact on production costs and the possibility of local production. Within this scope, accurate prediction of process loads during the machining operations plays a central role with respect to the exploration of design solutions and processing strategies while maintaining the necessary product quality. For this purpose a mechanistic model, based on the unified cutting mechanics theory, was developed for the prediction of cutting forces in face milling using inserted cutters, for the machining of ductile spheroidal cast iron. Ductile cast iron alloys are particularly prone to generate segmented chips. The applicability range of the fundamental model, the shear plane model underlying the unified mechanics of cutting, was studied for this phenomenon. A method was proposed to analyse chip segmentation and extract relevant data for the model implementation. Through experimental validation, it was proved that mechanistic models are a reliable option for modelling machining operation even under chip segmentation conditions.

© 2018 The Authors. Published by Elsevier Ltd.

This is an open access article under the CC BY-NC-ND license (<https://creativecommons.org/licenses/by-nc-nd/4.0/>)

Selection and peer-review under responsibility of the International Scientific Committee of the 8th CIRP Conference on High Performance Cutting (HPC 2018).

Keywords: Cutting Force Prediction; Chip Segmentation

1. Introduction

The purpose of the current research was to develop a model for cutting force prediction for face milling of spheroidal cast iron components. The model was a mechanistic model, based on the unified mechanics of cutting theory developed by Armarego [1], and it was intended to be used in combination with other algorithms to realize a tool path optimization procedure. Nodular ductile cast iron is a structural material whose popularity has

increased in recent decades, particularly in the wind power industry due to its mechanical properties and to the possibility of manufacturing mechanical components of high geometrical complexity and/or size. The microstructure peculiarity of these alloys radically influences the mechanical and thermal properties as well as their machinability. It is commonly known that cast iron alloys produce a segmented or discontinuous type of chip. The present paper reports a study on the impact of the peculiar segmented chip formation of ductile cast iron on cutting force

modelling. Chip segmentation in metal cutting was largely studied for titanium alloys and tool steel grades by various authors [2], [3]. It has been proved that the shear plane model is not a good representation of chip formation when segmentation occurs, as the deformation is not applied homogeneously to the entire engaged area of the workpiece material. Formulations to apply more consistently the shear plane model also in the case of segmented chip were proposed [4], [5]. Several authors used the same mechanistic approach to predict cutting forces in milling operations when cutting workpiece materials characterized by chip segmentation, proving good agreement between measurements and prediction [6]–[8]. However, the latter studies were conducted using relatively small values of feed per tooth and segmentation phenomena are less pronounced in these conditions, as proved by other studies [5], [9]. The present work therefore explores the possibility of applying the convenient simplification of a shear plane model in combination with the mechanistic model approach to the case of ductile cast iron, which is known to be characterised by segmented chip formation.

2. Mechanistic model features

The unified mechanics of cutting theory makes it possible to discretize a generic cutting edge into infinitesimal linear segments and to consider each of these segments as an oblique cutting operation [1], see Fig. 1. From this, a differential cutting edge that produces an uncut chip area dA and length db yields elemental cutting forces components as described in Eq. (1).

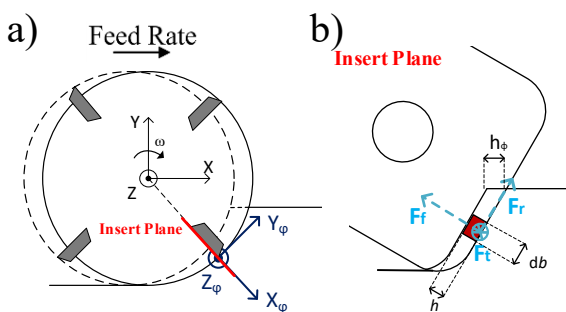


Fig. 1. (a) Reference system implemented in the cutting force model, referring to the forces acting on the tool; (b) Schematic representation of the insert's cutting edge discretization, and relative cutting forces.

$$dF_i = K_{i_c} * dA + K_{i_e} * db \quad (1)$$

where dA is the local uncut area, and can be expressed as $dA = h * db$, with h local uncut chip thickness and db is the differential length of the cutting edge. The cutting coefficients K_{i_c} are calculated using the oblique transformation method, Eq. (2-4), while the edge coefficients, K_{i_e} , are extrapolated from the cutting forces as intercept at zero uncut chip thickness. Ploughing phenomena or other effects occurring at the cutting edge are not modelled. The chip flow angle, η_c , and the normal friction angle, β_n , are determined numerically through the hypothesis of collinearity between the chip velocity and the friction force [6]. The lead angle for each elemental cutting edge

was described as function of the cutter geometric characteristics (radial and axial rake angle) [10], and as function of the insert geometry. The uncut chip thickness engaged by each elemental cutting edge was modelled as described by Armarego and Samaranyake [10]. Run-out was not implemented in the model.

$$K_{tc} = \frac{\tau * (\cos(\beta_n - \alpha_n) + \tan(i) * \tan(\eta_c) * \sin(\beta_n))}{\sin(\phi_n) * \sqrt{\cos^2(\phi_n + \beta_n - \alpha_n) + \tan^2(\eta_c) * \sin^2(\beta_n)}} \quad (2)$$

$$K_{fc} = \frac{\tau * \sin(\beta_n - \alpha_n)}{\sin(\phi_n) * \cos(i) * \sqrt{\cos^2(\phi_n + \beta_n - \alpha_n) + \tan^2(\eta_c) * \sin^2(\beta_n)}} \quad (3)$$

$$K_{rc} = \frac{\tau * (\cos(\beta_n - \alpha_n) * \tan(i) - \tan(\eta_c) * \sin(\beta_n))}{\sin(\phi_n) * \sqrt{\cos^2(\phi_n + \beta_n - \alpha_n) + \tan^2(\eta_c) * \sin^2(\beta_n)}} \quad (4)$$

3. Experimental procedures

3.1. Orthogonal Cutting experiments

Cutting coefficients K_{i_c} and K_{i_e} were calibrated by carrying out orthogonal cutting experiments, as described by Budak et al. [6]. Cutting forces and chip thickness values were measured in order to characterize the unknown variables in Eq. (2-4) shear stress on the shear plane, τ , the friction angle, β , the shear plane angle ϕ_n . Chip thickness is not constant when chip segmentation occurs. This has an impact in the definition of the unknown variables necessary to the model calibration. For this reason both the maximum chip thickness and the average chip thickness are measured and two calibrated versions of the model are created. Regarding the calculation of the friction angle β , average values of the cutting forces were chosen as representative. Orthogonal cutting tests were carried out over a reasonable range of the most relevant cutting parameters, the uncut chip thickness, the cutting speed and the rake angle. The values of the three parameters that were tested are listed in Table 1. A full factorial approach was used. The workpiece material machined was a nodular ductile cast iron of EN-GJS-400-18-LT grade, fully ferritic. Discs of 3 mm in width and 100 mm in diameter were cut from bars for orthogonal cutting tests. The cutting tool for holding the insert was custom-made, designed as part of a previous project [11]. The cutting insert used was the Tungaloy SPKN42STR carbide insert, PVD coated with TiAlN. The chips were collected and their thickness was measured using an optical CMM, specifically the Schut Geometrical Metrology DeMeet 220. Cutting forces were measured with the Kistler 9129AA dynamometer. The edge forces are identified by extrapolating the cutting forces to zero uncut chip thickness.

Table 1. Cutting parameters tested in orthogonal cutting experiments

Parameters	Values
Uncut chip thickness [mm]	0.01, 0.03, 0.05, 0.1, 0.2, 0.3, 0.4, 0.5
Cutting speed [m/min]	150, 200, 275
Rake angles [°]	-6, 5, 10

3.2. Face Milling Tests

Milling tests were carried out on a general CNC machine, Cincinnati 750 arrow 2, to validate the model prediction. The

indexed tool was a Sandvik Coromant hr262.2, on which Ceratizit TPKN 1603PPER inserts, PVD coated with TiAlN, were mounted. The axial rake angle is 5° , while the radial rake angle is 0° . Cutting forces were measured with the same equipment used for the orthogonal cutting tests. The workpiece material used was derived from the same cast iron bars used for the orthogonal cutting tests. The main cutting parameters are shown in Table 2. The tests were performed in down-milling configuration.

Table 2. Cutting parameters used for milling tests

Parameters	Values
Tool Diameter [mm]	50
Axial Depth of cut, A_p [mm]	1, 2, 3
Radial Depth of cut, A_e [%]	60, 100
Cutting Speed [m/min]	200
Feed rate [mm/tooth]	0.1, 0.2, 0.3, 0.4

4. Results and Discussion

During milling, the chip thickness is not a constant value, therefore chip segmentation may affect differently the model prediction. Chip segmentation occurs with various degrees depending on the cutting parameters and conditions. From the orthogonal cutting experiments it is found that the segmentation

increases with the uncut chip thickness, as also proved by other authors [5], [9]. The chip appears almost completely discontinuous at feed rate of 0.5 mm/rev, while at feed rate lower than 0.1 mm/rev the segmentation is not significant, see Fig. 2(a). In Fig. 2(b) it is shown how the choice of the chip thickness affects the shear angle. The shear plane model relation has been used considering both the maximum chip thickness and the average chip thickness, calculated considering the maximum chip thickness and the minimum chip thickness within a segmentation period, see Fig. 2(a). As can be seen in Fig. 2(b) at higher values of the uncut chip thickness the difference between the shear angle values calculated with the two methods increases. Specifically,

when the average chip thickness is used, the resulting shear angle is higher. The force coefficients dependency on the shear angle ϕ_n is described by Eq. (2)-(4). Here, the shear plane angle affects also the calibration of the shear plane stress, τ , which also contributes to the calculation of the force coefficients. A sensitivity analysis of the cutting coefficient $K_{t,c}$ in respect to the two different methods of calculating the shear angle ϕ_n is carried out and shown in Fig. 2(c). It is observed that the cutting coefficient $K_{t,c}$ as function of the uncut chip thickness is larger when the maximum chip thickness is chosen as the parameter that defines the shear angle.

Predicted milling forces obtained from considering the maximum chip thickness and the average chip thickness are compared to the measured milling forces in different engagement conditions, see Fig. 3. Respectively the engagement conditions are: $A_e = 60\%$, $A_p = 1$ mm, $f_z = 0.4$ mm/tooth, see Fig. 3 (a), $A_e = 100\%$, $A_p = 3$ mm, $f_z = 0.3$ mm/tooth, see Fig. 3 (b), and $A_e = 60\%$, $A_p = 2$ mm, $f_z = 0.1$ mm/tooth, see Fig. 3 (c). Cutting forces shown in Fig. 3 are the forces acting on the tool, reference system in Fig. 1. In general, there was good agreement between measurement and predictions, as the kinematics of the machining operation appears well described. Given the considerations expressed above, it is expected to observe a difference between the two model outputs when the uncut chip thickness is higher, therefore for higher feed rate. It is observed that for all the three cases shown in Fig. 3, the forces predicted when considering the maximum chip thickness to calculate the shear plane angle are higher, in absolute value, than the forces predicted when the average chip thickness is considered, accordingly to the behaviour of the cutting coefficient shown in Fig. 2 (c). This is most evident when the tooth engagement is maximum and/or when the overall feed rate is higher. Fig. 3 (c) shows an engagement condition with relative low feed per tooth. Considering the force F_y , as example, at the maximum chip engagement in one tool rotation the relative difference between

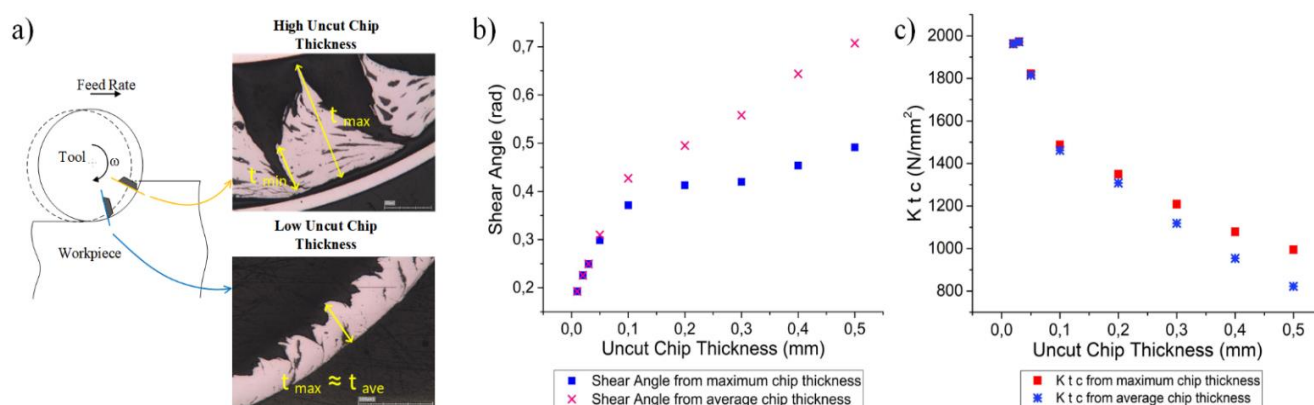


Fig. 2: (a) metallographic images of the chip section are shown to report the difference in chip segmentation that occurs for different feed per tooth values. (b), (c) the graph shows the variation of the shear angle and of the cutting coefficient $K_{t,c}$ respectively when the maximum or the average chip thickness are considered. $K_{t,c}$ is calculated for a rake face angle of -6° and an oblique angle of 15°

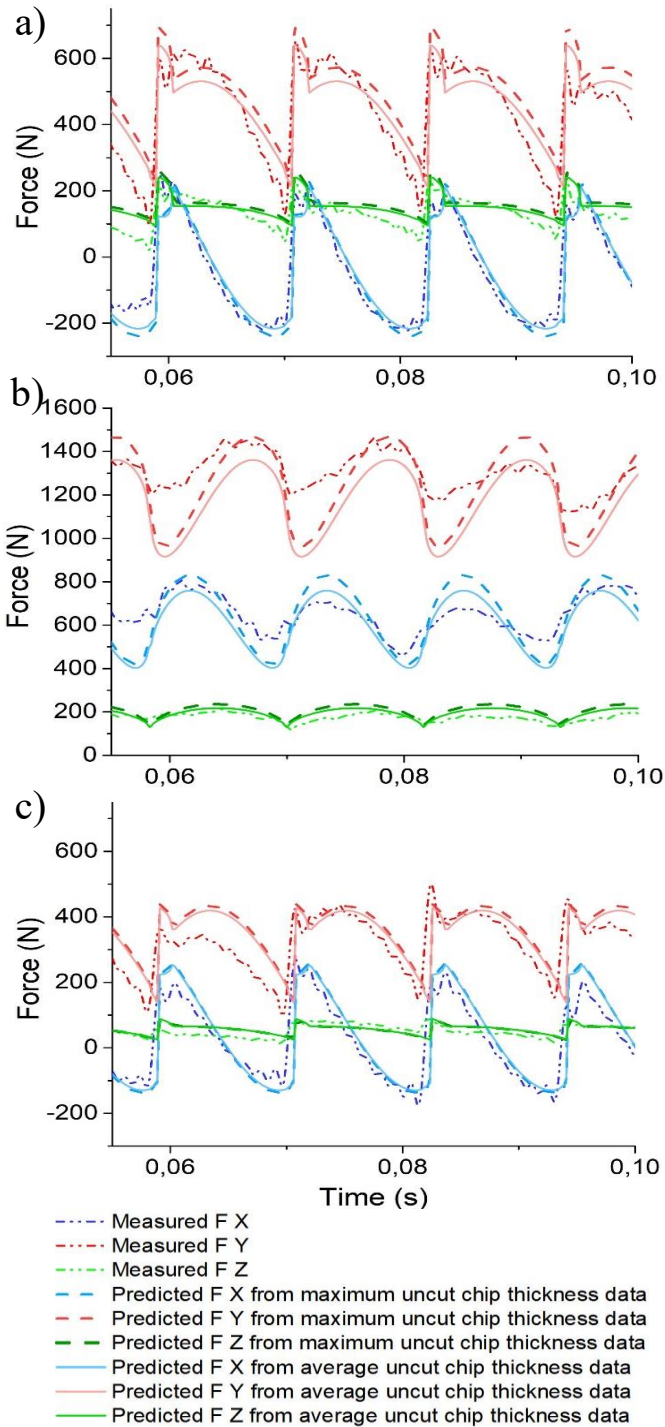


Fig 3: Comparison between measured and predicted of cutting forces acting on tool. Predicted forces are calculated following two approaches, considering the maximum or the average chip thickness. Engagement conditions shown are: (a) $A_e = 60\%$, $A_p = 1$ mm, $f_z = 0.4$ mm/tooth, (b) $A_e = 100\%$, $A_p = 3$ mm, $f_z = 0.3$ mm/tooth, (c) $A_e = 60\%$, $A_p = 2$ mm, $f_z = 0.1$ mm/tooth. Tool diameter = 50 mm.

the two approaches in the case of Fig. 3 (c) is 5.9%, while in the other two cases, respectively Fig. 3 (a) and Fig. 3 (b), are 12.6%

and 14.5%. Similar trends regarding the relative differences were observed also for the other cutting forces.

5. Conclusions

The mechanistic model presented in this work is capable of accurately predicting the cutting forces in a face-milling operation with an inserted cutter, across widely different engagement conditions. As first approximation, the shear plane angle characterization can be carried out considering the maximum chip thickness as it does not introduce significant errors in the prediction of the cutting forces and as it does not require time-consuming metallographic procedures. Also, it is observed that those errors are variable as function of the process parameters, being larger for larger values of the radial engagement and the feed rate. A reliable force prediction employing mechanistic models can be obtained also in case of segmented chip, therefore considerably simplifying the model calibration procedure.

Acknowledgements

The research studies presented in this article were carried out as part of the Innomill project, in part funded by the Innovation Fund Denmark.

References

- [1] E. J. A. Armarego, "The unified-generalized mechanics of cutting approach—a step towards a house of predictive performance models for machining operations," *Mach. Sci. Technol.*, vol. 4, no. 3, pp. 319–362, Nov. 2000.
- [2] M. C. Shaw and A. Vyas, "The Mechanism of Chip Formation with Hard Turning Steel."
- [3] R. Komanduri and B. F. Von Turkovich, "New observations on the mechanism when machining titanium alloys of chip formation," *Wear*, vol. 69, no. 2, pp. 179–188, 1981.
- [4] P. L. B. Oxley, *The Mechanics of Machining: An Analytical Approach to Assessing Machinability*. Ellis Horwood, 1989.
- [5] B. Lindberg, B. Lindström, and T. Royal, "Measurements of the Segmentation Frequency in the Chip Formation Process," *Ann. CIRP*, vol. 32, pp. 17–20, 1983.
- [6] E. Budak, Y. Altıntaş, and E. J. A. Armarego, "Prediction of Milling Force Coefficients From Orthogonal Cutting Data," *J. Manuf. Sci. Eng.*, vol. 118, no. 2, p. 216, 1996.
- [7] Y. Altıntaş and P. Lee, "A General Mechanics and Dynamics Model for Helical End Mills," *Ann. CIRP*, vol. 45, no. 1, 1996.
- [8] G. Yücesan and Y. Altıntaş, "Improved modelling of cutting force coefficients in peripheral milling," *Int. J. Mach. Tools Manuf.*, vol. 34, no. 4, pp. 473–487, 1994.
- [9] C. Courbon, T. Mabrouki, J. Rech, D. Mazuyer, F. Perrard, and E. D'aramo, "Further insight into the chip formation of ferritic-pearlitic steels: Microstructural evolutions and associated thermo-mechanical loadings," *Int. J. Mach. Tools Manuf.*, vol. 77, pp. 34–46, 2013.
- [10] E. Armarego and P. Samaranayake, "Performance prediction models for turning with rounded corner plane faced lathe tools. II. Verification of models," *Mach. Sci. Technol.*, vol. 3.2, pp. 173–200, 1999.
- [11] G. Bissacco, "Surface Generation and Optimization in Micromilling," DTU, 2004.